Metal Current Collector for LMBs

Subjects: Chemistry, Applied
Contributor: rajesh pathak

Lithium Metal Anode (LMA) has been considered as the promising candidate, owing to their high theoretical gravimetric capacity, low electrochemical potential, and low density, to replace the conventional carbon based anode materials of lithium-ion batteries (LIBs). Unfortunately, the inherent hyperactive and volume expansion issues of Lithium (Li) leads to the formation of notorious Li dendrite growth and unstable solid-electrolyte-interphase (SEI), eventually hindering the practical application of lithium metal batteries (LMBs). To resolve this issue, one of the effective approach is to engineer three dimensional (3D) porous metal based Li host owing to their chemical and mechanical stability, high electronic conductivity and low cost. In this review, the challenges and strategies to suppress the Li dendrite growth are presented. Then the design principles and effectiveness of different kinds of metal based Li host to accommodate and buffer the volume expansion of Li for guiding the uniform Li deposition are summarized. Then the special attention is paid to the lithiophilic coating or decoration which can further control the initial Li deposition and lowers the nucleation and voltage overpotential in 3D porous metal framework during Li plating/stripping cycles. Finally, the conclusion and perspective are given on the current status, challenges and future research pathway toward advancement of LMA for dendrite-free and improved battery performance.

Keywords: lithium metal batteries (LMBs), ; three-dimensional (3D) metal porous framework ; lithiophilic coating or nano-seed decoration ; Dendritre-free Li deposition ; improved cycling performance

---

The electrochemical stability of the metal must be taken into account before using it as the Li host in LMBs [1]. To host the Li anode, the challenge is with Li alloying at a low potential range of 0.01–2.0 V versus Li/Li^+. Copper (Cu), nickel (Ni), and stainless steel are considered stable enough to be used as Li host materials. The initial plating of lithium on planar two dimensional (2D) substrate renders inhomogeneous Li deposition due to the inhomogeneous distribution of the electric field. The rough, cracks, and inhomogeneous Li nucleation act as hot spots, which favor the continuous deposition of Li leading to dangerous Li dendrites and mossy Li. The continuous growth of needle and whisker shaped Li dendrite growth not only challenges the safety concern of batteries but also leads to the formation of uncontrolled and undesired formation/deformation of SEI. Thus, a host with abundant Li storage sites is strongly recommended, which can provide the route for dendrite free Li deposition and accommodate the volume expansion of Li, during Li plating/stripping, even at higher current density.

1. Lithium

Lithium metal itself can be constructed as the Li host in the form of a nano/microstructured framework. Ryou et al. designed defects in the lithium foil using the microneedle technique shown in Figure 1a to introduce high surface areas that serve as preferred sites for Li plating [2]. The other methods of producing microstructured Li include soft lithography, where continuous surface relief (CSR) and discontinuous surface reliefs (DSR) were fabricated on the surface of the Li metal foil electrode [3]. The continuous and discontinuous 10 μm deep surface modifications on 20 μm thin Li electrode as shown in Figure 1b,c provides an effective way to replace the use of excess Li. Kong et al. pressed the Li powder with a particle size of fewer than 20 μm on stainless steel mesh Figure 1d to create a porous Li-powder anode [4]. The porous anode with 25% Li loading eliminates the growth of Li dendrites. Later, Park et al., introduced micropatterns on lithium metal using micrometer-scale pyramid reliefs (height-50 μm, width-50 μm, and ridge length-40 μm) [5]. During stripping, the original dimension was recovered draining the liquid-like/or granular like plated Li from such structures as shown in Figure 1e,f. The coating of the micrometer particle size Li powder (CLiP) on the copper foil as shown in Figure 1g can also be done to improve the battery performance and replace the excess Li foil electrode [6]. This study shows that the porous structure and high surface area of the coated/pressed Li powder significantly reduce the current density during plating/stripping. The CLiP introduced the safety and practical battery operation at a lean lithium condition.

To further enhance the self-healing electrostatic shield mechanism, Kim et al., employed an electrolyte solution containing cesium hexafluorophosphate $CsPF_6$ (0.05 M) into micropatterned LMA [7]. The cesium ions form a positively charged electrostatic shield around the initial growth of protrusions, which obliges the deposition of Li adjacent to the protrusions

leading to dendrite-free Li deposition [8][9]. Figure 1h,i show the cross-section SEM image of micropatterned Li without and with $CsPF_6$. The micropatterned Li metal shows the uncontrolled granular Li deposition. In contrast, the micropatterned Li with $CsPF_6$ modifications shows the dendrite-free and stabilized Li metal anode.

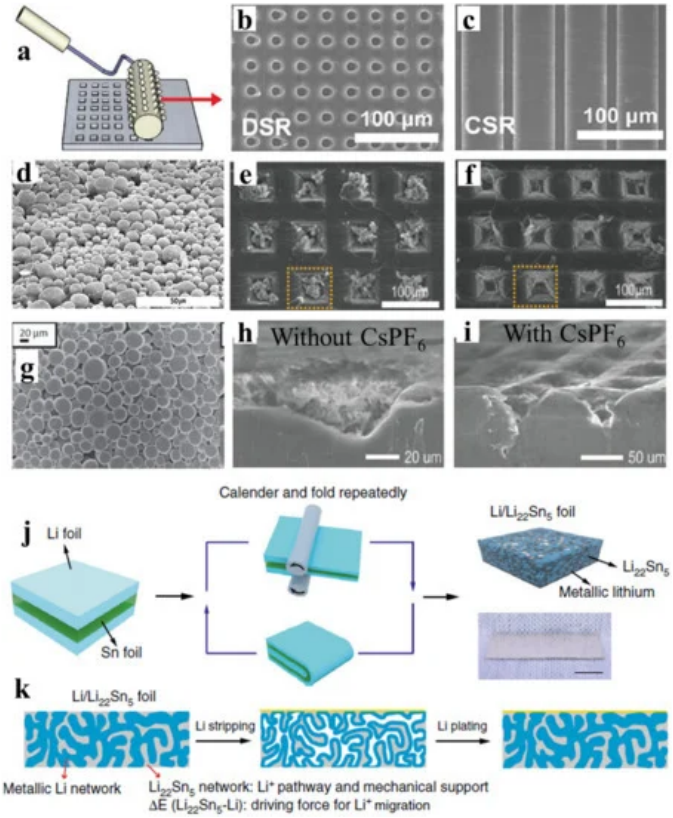

Figure 1. Micropattern preparation process and Li deposition morphology on porous Li. (**a**) Schematic demonstration of the microneedle technique. Reproduced with permission from [2], John Wiley and Sons, 2014. (**b**,**c**) SEM images of continuous surface relief (CSR) and discontinuous surface relief (DSR) on the Li electrode. Reproduced with permission from [3], American Chemical Society, 2019. (**d**) SEM image of the Li-powder electrode. Reproduced with permission from [4], Institute of Physics Publishing, 2012. (**e**,**f**) SEM images of Li plated and stripped. Reproduced with permission from [5], John Wiley and Sons, 2016. (**g**) SEM image of the coating of the micrometer particle size Li powder (CLiP) electrode**.** Reproduced with permission from [6], John Wiley and Sons 2013. (**h**,**i**) Cross-section SEM images of patterned Li without and with $CsPF_6$. Reproduced with permission from [7], Elsevier, 2018. (**j**,**k**) Schematic illustration of the preparation and Li plating/stripping on the Li/Li-Sn composite electrode. Reproduced with permission from [10], Springer Nature, 2020.

The battery operation at a higher rate demands low effective current density and fast lithium-ion diffusion kinetics. The nanostructured electrode lower effective current density and the lithium-containing alloys can facilitate the faster lithium-ion diffusion. Recently, Wan et al. reported an interpenetrated 3D lithium metal/lithium tin alloy nanocomposite by a simple calendaring and folding route and lithium-tin alloying reaction mechanism as shown in Figure 1j [10]. The schematic of dendrite-free Li deposition during plating/stripping cycles achieved with such lithium and the lithium-tin alloy is shown in Figure 1k. The strong anchorage affinity between lithium and lithium–tin alloy leads to low interface impedance and dense structure [11]. The potential difference between lithium and lithium–tin alloy and abundant interfaces enable ultrafast Li-ion diffusion across the entire LMA electrode. As a result, the lithium metal/lithium tin alloy nanocomposite anode delivered stable lithium plating/stripping cycles at 30 mA cm^{-2} and 5 mAh cm^{-2} for 200 cycles. The full cell configuration with $LiNi_{0.6}Co_{0.2}Mn_{0.2}O_2$ (NCM) cathode exhibited an outstanding rate capability of 74% at 6 C compared to its initial capacity (167 mAh g^{-1} at 0.5 C) and with $LiFePO_4$ (LFP) cathode demonstrated capacity retention of 91% at 5 C after 500 cycles, respectively.

2. Copper

The 3D nanostructured copper with a high electroactive surface area is considered as an appealing Li host matrix. Such a framework can lower the current density and provide the room to accommodate the Li and manipulate the electric filed for guiding the Li deposition. To synthesize 3D Cu porous nanostructure, Yang et al. reported the simple solution-based approach with a submicron framework (median pore size 2.1 μm) by immersing the planar Cu foil in ammonia solution [12]. Figure 2a shows the schematic representation of preparing 3D porous Cu from the planar Cu. Figure 2b shows the lithium-ion flux in planar and 3D porous Cu. In planar Cu, the irregular, rough, and cracks act as a local hotspot for Li-ion

accumulation. The Li metal deposition is amplified at those Li-ion accumulation centers with higher plating cycles, which leads to the growth of Li dendrites. The high surface area of Li dendrite consumes an excess amount of electrolyte and Li leading to poor CE and quick capacity fading. Besides, the dendritic Li can pierce the separator, which can cause a short circuit or fire caught, threatening the safety concern of batteries. In contrast, 3D porous Cu has uniformly distributed the Li-ion flux due to the numerous and uniform protuberant tips on the submicron fibers. As a result, the deposited Li fills the pores evenly without any Li dendrites. The high pore volume of the structure can provide sufficient room to accommodate Li that leads to the stable and reversible Li plating/stripping. As a result, the 3D porous Cu showed plating/stripping cycles for 600 h with low voltage hysteresis (<50 mV) at 0.2 mA cm^{-2} and exhibited a CE of 98.5% at 0.5 mA cm^{-2}. Further Li deposition behavior study on 3D Cu foam with an average pore size 170 µm showed that Cu foam does not have any effect of the Li space constraint. This led to the Li metal detachment from the backbones of the Cu foam causing electric disconnection, which induces Li dendrite growth. Lu et al. reported a free-standing 3D Cu nanowire (CuNW) network membrane via reducing copper nitrate in the NaOH aqueous solution [13]. The voltage hysteresis was further lowered to 40 mV and the CE, which reached 99.2% after 50 cycles remain stable to 98.6% after 200 cycles at 1 mA cm^{-2}. The full cell coupled with the $LiCoO_2$ cathode shows an outstanding 30% increase in the specific capacity at 5 C indicating the advantage of the Li-CuNWs nanocomposite in LMBs at a higher rate.

The dealloying mechanism such as the dissolution of zinc (Zn) out of brass (Cu-Zn alloy) using various chemical-solution and vacuum distillation processes results in the formation of voids and microstructures [14][15][16]. The porosity can be easily tuned by adjusting the etching condition (such as the concentration of the solution, distillation temperature, and time) depending upon the method used. The interconnected, uniform, and smooth porous Cu provides sufficient electrical conductivity, uniform Li-ion flux, and space for Li accommodation. Besides, 3D porous Cu exhibited the lower voltage hysteresis as shown in Figure 2c,d, and improved cycling performance with a capacity retention of 87.2% after 300 cycles of charge/discharge at 50 mA g^{-1} as shown in Figure 2e [15][16].

The vertically distributed electric field promotes the vertical growth of Li dendrites, which continues to grow towards the separator and cathode and eventually pierce the separator causing short-circuits. To address these issues, it is necessary to constrain the lithium dendrite growth within the porous scaffold and distribute the electric field in the lateral direction. For this, the compartmented and the vertically aligned (VA) 3D porous Cu have been designed by the laser microprocessing system, and a series of processes, including hot lamination, laser ablation, and alkaline etching treatments. Zou et al. developed compartmented 3D Cu (150 µm diameter) by an industry-adaptable technology following a series of processes, including hot lamination, laser ablation, and alkaline etching treatments [17]. The insulating polyimide (PI)-clad copper grid with lateral electric field distribution designated as E-Cu guides the Li deposition laterally within the porous scaffold of Cu (Figure 2f,g). In contrast, pristine copper (P-Cu) showed larger, thicker dendrites with an uneven surface as shown in Figure 2h,i. Wang et al. used a laser microprocessing system to design VA microchannels with optimized pore radius, pore depth, and pore spacing of 5 µm, 50 µm, and 12 µm, respectively [18]. The VA porous Cu provides a large surface area to deposit the lithium in the microchannels as shown in Figure 2j,k. The VA porous Cu demonstrated a stable CE of 98.5% for 200 cycles and voltage hysteresis of 30 mV after 50 cycles [18]. The lithium deposited porous Cu anode paired with the $LiFePO_4$ (LFP) cathode demonstrated higher capacity retention of 90% compared to the planar Cu (80%) after 100 cycles at 0.5 C.

The other techniques such as mechanical press or folding techniques have also been reported to make a 3D Cu/Li-metal composite anode that demonstrated a high CE and a longer and ultra-high plating/stripping capacity up to 50 mAh cm^{-2} at an ultrahigh current density of 20 mA cm^{-2} [19][20]. Cao et al., developed the vertically oriented lithium–copper–lithium arrays composite anode developed by mechanical rolling or repeated stacking [20]. Such composite anode showed voltage hysteresis of less than 55 mV and a lifetime up to 2000 h at 1 mA cm^{-2} to achieve a capacity of 1 mAh cm^{-2}.

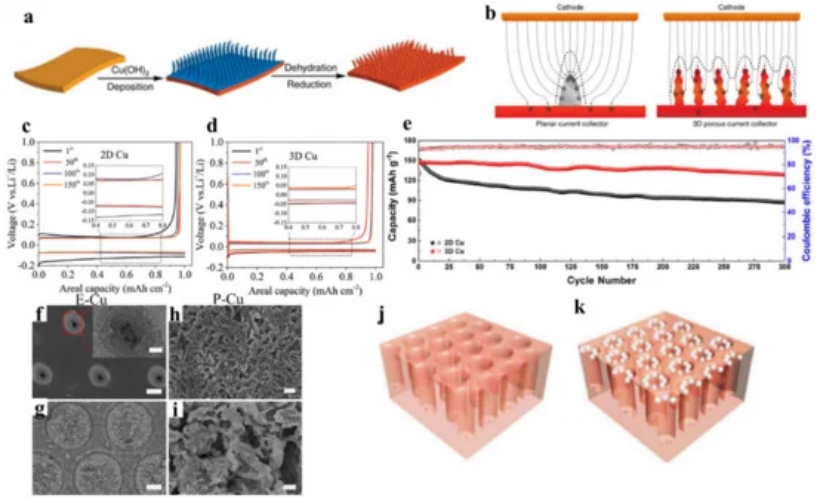

Figure 2. The lithium deposition behavior of Cu based porous framework. (**a**,**b**) Schematic illustration to prepare 3D porous Cu foil from planar Cu foil and the Li-ion flux distribution on planar and 3D Cu current collector. Reproduced with permission from [12], Springer Nature, 2015. (**c**,**d**) The comparison of the voltage profile of Li plating/stripping on 2D and 3D current collectors at a current density of 1 mA cm^{-2} to reach a capacity of 1 mAh cm^{-2}. Reproduced with permission from [15], John Wiley and Sons, 2018. (**e**) The comparison of cycling performance of a Li anode with 2D and 3D Cu current collector paired with the $(NiCoMn)O_2$ cathode. Reproduced with permission from [21], Elsevier, 2018. (**f**) Top-view SEM image of E-Cu after cycling of 150 cycles at 0.5 mA cm^{-2}; inset shows the magnified image of the pinhole. (**g**) Top-view SEM image of E-Cu after peeling off the upper PI film. (**h**) Top-view SEM image of P-Cu after cycling. (**i**) Magnified top-view SEM image from the selected area in **c.** The scale bars in (**f**–**i**) are 50 µm, 50 µm, 2 µm, and 500 nm, respectively. The scale bar in the inset of (**f**) is 10 µm. Reproduced with permission from [17], Springer Nature, 2018. (**j**,**k**) Schematic of the vertically aligned (VA) porous Cu and the Li deposition preferential on it. Reproduced with permission from [18], John Wiley and Sons 2017.

The poor wettability of lithium towards Cu does not spread the molten Li across the surface of lithiophobic substrates, promoting the non-uniform and dendritic Li deposition. To overcome this problem, the lithiophobic surface of Cu can be converted to lithiophilic by various coatings or layers of metal [22][23], oxide [24][25][26][27][28][29], nitride [28][29], oxynitride[30], sulfide[31], and phosphide [32], the addition of functional groups or doping [33][34][35][36][37][38], and by an increase in temperature [39].

Wang et al., studied the tuning of Li wettability by reacting molten lithium with elemental additives and organic compounds containing functional groups [37]. The negative value of Gibbs formation energy ($\Delta_f G$) for the reaction between the molten Li and coated/doped compounds indicates the formation of a new chemical bond, which improves the Li wettability. The wettability of Li was improved by adding elements such as indium (In), tin (Sn), and magnesium (Mg), which reduces the surface tension of the material and spread the lithium. Figure 3a shows the periodic table indicating the electronegativities and Li wettability strength of elements. The reaction of molten Li and the elements form a new chemical bond responsible for improving Li wettability. The coating of an organic compound containing -OH, $-SO_3H$, $-NH_2$, -NH, $-PO_4$, -Si-O, -F, -Cl, -Br, or -I on the surface of lithiophobic substrate is another strategy to improve the Li wettability. The successful enhancement in the lithiophilic property of porous framework, based on chemical strategy between Li and lithiophilic coating, can enable the development of ultrathin Li anodes.

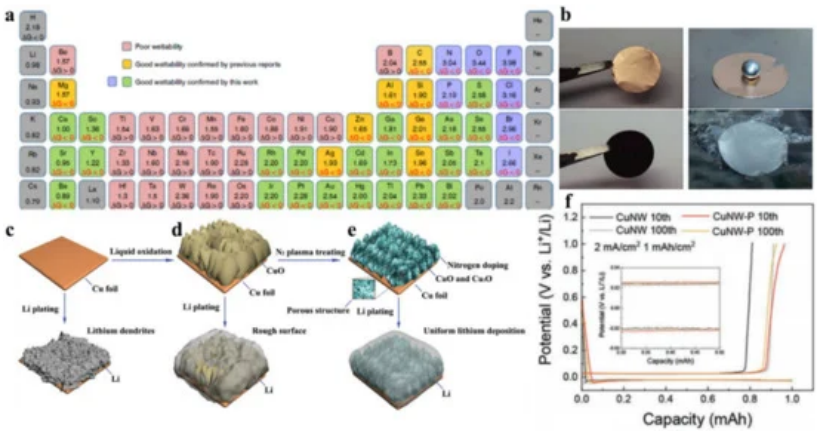

Figure 3. Lithiophilic behavior on the Cu based porous framework. (**a**) Electronegativities of the various elements and $\Delta_f G$ of elements/compounds reacted with the molten Li. Reproduced with permission from [37], Springer Nature, 2019. (**b**) Li wettability on the surface of Cu foil and VA-CuO-Cu substrate. Reproduced with permission from [28], John Wiley and Sons, 2018. (**c**–**e**) Schematic representation of the Li plating mechanism on planar Cu, VA-CuO-Cu, and nitrogen-doped VA-CuO and Cu_2O-Cu. Reproduced with permission from [26], John Wiley and Sons, 2019. (**f**) Charge/discharge voltage profiles of the CuNW and CuNW-P collectors after 10 and 100 cycles at a current density of 2 mA cm^{-2} for a total capacity of 1 mAh cm^{-2} of Li. Reproduced with permission from [34], John Wiley and Sons, 2019.

Zhang et al., reported thin lithiophilic CuO VA nanosheets grown on Cu substrate by a simple wet chemical reaction, which not only ensures the good electrical conductivity of the electrode but also facilitates the fast Li-ion transport and regulates the Li nucleation [28]. Figure 3b shows that the molten Li is uniformly spread out on the VA-CuO-Cu surface but the molten Li forms a droplet on the Cu surface confirming the lithiophilicity and lithiophobicity of the VA-CuO-Cu surface and Cu surface, respectively. To further enhance the lithiophilic property, the dual lithiophilic materials can be employed. The lithiophilic copper oxides were grown on Cu foil by liquid oxidation of bare Cu foil and the subsequent N_2 plasma treating to achieve a high CE of 99.6% for 500 cycles at 1 mA cm^{-2} for 1 mAh cm^{-2} capacity [26]. The symmetrical cell demonstrated long cycling of more than 600 h with a low voltage hysteresis of 23.1 mV. This can be attributed to the regulated Li nucleation and reduced overpotential for guiding dendrite-free Li deposition. Figure 3c–e clearly demonstrated that the plasma strengthened CuO/Cu_2O decorated Cu showed the uniform morphology of deposited Li. For the dense nucleation of Li and steady deposition into the porous structure, the copper nanowire with a phosphidation gradient (CuNW-P) was prepared by the chemical solution process first to grow CuNW and the subsequent chemical vapor reaction to generate phosphine gas [34]. A high Li loaded (44%) CuNW-P demonstrated a significant decrease in the nucleation overpotential and voltage hysteresis as shown in Figure 3f.

3. Nickel

Similar to the 3D porous Cu, the 3D porous Ni has also been considered as a better alternative to any 2D Li host. The 3D structure incorporates the active anode material and provides efficient charge transport pathways. To improve the high rate capability, cyclability, and reduce the lithium amount, the foam lithium anode was prepared by Li electrodeposition on a Ni foam substrate [40]. Developing the honeycomb-like porous 3D Ni host on the Cu current collector via a hydrogen bubble dynamic template electrodeposition method has also been reported for stable Li and Na metal batteries [41]. However, the electrochemical deposition of lithium into the Ni foam host material for making Li/3D Ni composite anode, generally, leads to uneven Li deposition. Moreover, the batteries have to be dissembled, cleaned, and further assembling of a new battery is needed for pairing the resultant composite electrodes with the practical cathode materials. To address this complex and costly process, the development of a simple approach for encapsulating Li inside porous Ni or other scaffolds to develop Li-based composite anode is highly looked-for.

Chi et al., reported the thermal infusion strategy for pre-storing molten Li into stable 3D Ni foam to achieve a composite anode [42]. Figure 4a shows the schematic illustration of making the Li/3D Ni foam composite anode. Figure 4b,c shows the digital photos of Ni foam and the Li-Ni composite. Figure 4d–f shows the SEM images of Ni foam and Figure 4g–i shows the corresponding SEM images after molten Li infusion. The molten lithium fills the large pores of the Ni foam and Ni frameworks protuberance marked with the yellow arrow still exist, which implies that the architecture was well preserved. The composite anode with 26 mg cm^{-2} loading of Li (50 wt % of composite) exhibited improved plating/stripping cycles for more than 100 cycles at 5 mA cm^{-2} in the carbonate-based electrolyte. This can be attributed to the significant reduction in the interfacial resistance and smooth Li deposition. After 100 cycles of plating/stripping, the irreversible Li plating on bare Li shows deposition of 90 µm thick Li, however, the Li-Ni composite anode does not show any thickness change. Moreover, the full cell configuration with composite anode demonstrated better rate capability, low interfacial resistance, and lower voltage overpotential compared to the bare Li anode.

To further address the issues of LMA and improve the electrochemical performance of LMBs, it is required to decorate the 3D Li host with lithiophilic coatings. The lithiophilic decoration in a porous Li host can greatly reduce the nucleation overpotential and guide the uniform Li deposition. To increase the affinity or Li wettability between the lithium and 3D porous host, various polymers [43], organic coating [37], elementary substances (such as Si nanoparticles [44], plated Ag [45]), oxides (such as NiO [46], CoO [47], Co_3O_4 [48], ZnO nanoarrays (NAs) [49]), fluorides (NiF_x) [50], nitrides (Ni_3N) [51], and sulfides (Ag_2S) [52] have been utilized.

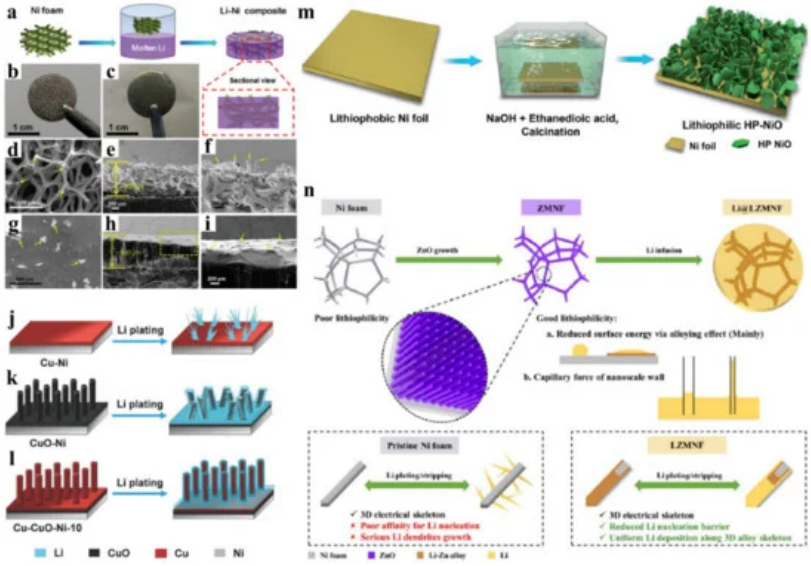

Figure 4. Lithiophilic behavior on the Ni-based porous framework. (**a**–**i**) Fabrication of the Li-Ni composite. Reproduced with permission from [42], John Wiley and Sons, 2017. (**j**–**l**) The schematic representation of Li plating on Cu-Ni, Cuo-Ni, and Cu-CuO-Ni. Reproduced with permission from [53], John Wiley and Sons, 2018. (**m**) Schematic illustration of HP-NiO sheets' growth on Ni foil. Reproduced with permission from [54], Royal Society of Chemistry, 2019. (**n**) The schematic illustration of lithiophilic ZnO NA modified Ni foam (ZMNF) growth and its advantages. Reproduced with permission from [49], Royal Society of Chemistry, 2019.

Wu et al., prepared a lithiophilic Cu-Cuo-Ni hybrid structure by depositing Cu on Ni foam by radio frequency (R-F) sputtering followed by annealing at 400 °C and then finally, CuO-Ni was reduced by H_2 plasma [53]. Figure 4j–l shows the lithium plating mechanism on Cu-Ni, CuO-Ni, and Cu-CuO-Ni current collector. The copper has high overpotential for Li nucleation, which can be lowered by using the lithiophilic CuO nanowire (NW) arrays. Besides, the evenly distributed electric field on CuO-NW arrays leads to the uniform Li-ion flux and lowers the current density. The thin layer of the Cu layer on CuO still maintains the lithiophilicity, offers lower nucleation potential, and increases the electrical conductivity. The Cu film acts as a protective layer during electrochemical cycling. As a result, the hybrid Cu-CuO-Ni structure demonstrated a dendrite free Li plating with CE > 95% for more than 250 cycles at 1 mA cm^{-2} and long symmetrical plating/stripping cycling up to 580 h at 0.5 mA cm^{-2} with a capacity of 0.5 mAh cm^{-2}. Lu et al. designed nanostructured lithiophilic VA NiO hexagonal nanoplates on Ni foil (HP-NiO-Ni) by a facile hydrothermal process as shown in Figure 4m [46]. Such a HP-NiO-Ni nanostructure significantly reduces the current density and nucleation overpotential for efficient, homogeneous, and smooth Li deposition. Besides, the lithiophilic Li_2O and electronic conductive Ni formed during the reversible conversion reaction of NiO to Ni/Li_2O facilitates uniform Li-ion transport and fast electron conduction pathways, respectively. Thus, the synergy of reversible conversion reaction, and the uniform/reversible Li plating mechanism stores excess Li even at higher current density.

The formation of the Li containing alloy is believed to lower the nucleation overpotential and guide the uniform Li deposition [11]. Sun et al. reported the lithiophilic ZnO NA modified Ni foam (ZMNF) by a facile seed-mediated hydrothermal reaction process [55]. The ZMNF current collector improved the affinity towards the Li, provided fast Li-ion kinetics, reduced the nucleation barrier, and lessened the Li volume expansion during plating/stripping cycles. The ZnO NA improves the Li affinity with molten Li by alloying and capillary effect as shown in Figure 4n. As a result, ZMNF exhibited a CE above 98% for over 300 cycles at 1 mA cm^{-2} and a symmetrical cell demonstrated a long plating/stripping cycles over 1200 h at 1 mA cm^{-2} to achieve 2 mAh cm^{-2}.

The graphene-based materials can provide scaffolds for Li electrodeposition and act as nucleation seeds. Graphitized carbon on Ni foam by heating Ni foam up to 1000 °C under Ar and H_2 and introducing methane (CH_4) [56] or acetylene (C_2H_2) [57], few-layered graphene sheets attached to the surface of Ni foam following the acid-catalyzed hydrothermal process [58] have been reported for reduced overpotential and improved battery performance.

The other metal-based current collector such as titanium (Ti) and stainless steel has also been reported to guide the uniform Li deposition in LMBs. Zhang et al. proposed a porous lightweight corrosion-resistance 3D Ti current collector, which achieved outstanding CE of 99% at 1 mA cm^{-2} to achieve a capacity of 5 mAh cm^{-2} [59]. The metal-based porous framework including the methods of preparation and electrochemical performance is summarized in Table 1.

Table 1. Summary of the metal-based porous framework in lithium metal batteries (LMBs).

Metal-Based Porous Framework	Methods/Modifications for Creating a Porous Structure	Electrochemical Performance	Ref.
Micropatterned-Li	Microneedle	Improved rate capability and cycling stability by 20% and 200%, respectively.	[2]
CSR/DSR Li	Lithography	Stable Li plating/stripping up to 10 mA cm^{-2} and improved cycling performance at 10 C	[3]
Micropatterned-Li	Pressing/coating of µm-sized Li powder	Cycling performance and dendrite-free Li deposition shows the possibility to replace anode with excess Li.	[4][6]
Micropatterned-Li	µm-scale pyramid reliefs	Reversible Li plating/stripping	[5]
Micropatterned-Li	Microneedle + $CsPF_6$ additive	Provides self-healing electrostatic shield	[7]
3D nanostructured-Li	calendaring and folding	20 mV overpotential for 200 cycles at 20 mA cm^{-2}	[10]
3D sub-micron sized Cu	ammonia solution process	<50 mV polarization after 600 h cycling, CE 98.5% at 0.5 mA cm^{-2}	[12]
3D CuNW	alkaline solution process	Plating of 7.5 mAh cm^{-2} of Li, CE 98.6% during 200 cycles at 1 mA cm^{-2}	[13]
3D porous Cu	Dealloying of brass–ammonium chloride solution process	CE 97% for 250 cycles at 0.5 mA cm^{-2}	[14]
3D porous Cu	Linear sweep voltammetry in acidic solution	20 mV polarization, stable 400 h plating/stripping at 1 mA cm^{-2}	[15]
3D porous Cu	Vacuum distillation-(400–900) °C	800 h plating/stripping at 0.52 mA cm^{-2}	[16]
Microcompartmented-Cu	hot lamination, laser ablation, and alkaline etching	CE 99% after 150 cycles at 0.5 mA cm^{-2}.	[17]
VA-microchannel-Cu	Laser microprocessing	20 mV polarization, CE 98.5 within 200 cycles at 1 at 1 mA cm^{-2}	[18]
3D porous Cu/Li-metal composite	mechanical press or folding	60 mV polarization, CE 93.8% after 100 cycles at 0.5 mA cm^{-2}	[19]
Vertically oriented Li-Cu-Li arrays	rolling-folding-winding	Deep charging up to 50 mAh cm^{-2}, 2000 h plating/stripping at 1 mA cm^{-2}	[20]
Ni-foam	Molten Li infusion	Stable cycling for >100 cycles with reduced hysteresis at 5 mA cm^{-2}	[42]
3D porous Ti	Directly purchased	CE 99% at 1 $mAcm^{-2}$	

To further enhance the lithiophilicity of Ti, the CuO nanoflower was grown on Ti mesh by the microwave-assisted solution reaction at 100 °C, which was further pressed on the Li wafer by a battery sealer with mechanical pressure of 800 psi [60]. The Li/Cuo@Ti-mesh (LCTM) composite anode exhibited a high CE of 94.2% at 10 mA cm^{-2} over 90 cycles with a low overpotential of 50 mV. The low overpotential of 50 mV and 250 mV were achieved at a high current density of 20 and 40 mA cm^{-2}. Lee et al., used the 3D conductive stainless steel fibrous metal felt (FMF) of a fiber diameter of 10 µm, porosity of 80%, and surface area or 0.05 m^2 g^{-1} to prepare the FMF/Li electrode by roll-pressing [61]. The FMF/Li symmetrical cell test showed a low overpotential of 30 mV at a high current density of 10 mA cm^{-2}.

References

1. Jin, S.; Jiang, Y.; Ji, H.; Yu, Y. Advanced 3D Current Collectors for Lithium-Based Batteries. Adv. Mater. 2018, 30, 1802014.
2. Ryou, M.H.; Lee, Y.M.; Lee, Y.; Winter, M.; Bieker, P. Mechanical surface modification of lithium metal: Towards improved Li metal anode performance by directed Li plating. Adv. Funct. Mater. 2015, 25, 834–841.
3. Ahn, J.; Park, J.; Kim, J.Y.; Yoon, S.; Lee, Y.M.; Hong, S.; Lee, Y.-G.; Phatak, C.; Cho, K.Y. Insights into Lithium Surface: Stable Cycling by Controlled 10 µm Deep Surface Relief, Reinterpreting the Natural Surface Defect on Lithium Metal Anode. ACS Appl. Energy Mater. 2019, 2, 5656–5664.
4. Kong, S.-K.; Kim, B.-K.; Yoon, W.-Y. Electrochemical behavior of Li-powder anode in high Li capacity used. J. Electrochem. Soc. 2012, 159, A1551–A1553.

5. Park, J.; Jeong, J.; Lee, Y.; Oh, M.; Ryou, M.H.; Lee, Y.M. Micro-Patterned Lithium Metal Anodes with Suppressed Dendrite Formation for Post Lithium-Ion Batteries. Adv. Mater. Interfaces 2016, 3, 1600140.
6. Heine, J.; Krüger, S.; Hartnig, C.; Wietelmann, U.; Winter, M.; Bieker, P. Coated Lithium Powder (CLiP) Electrodes for Lithium-Metal Batteries. Adv. Energy Mater. 2014, 4, 1300815.
7. Kim, S.; Choi, J.; Lee, H.; Jeong, Y.-C.; Lee, Y.M.; Ryou, M.-H. Suppression of dendrites and granules in surface-patterned Li metal anodes using CsPF6. J. Power Sources 2019, 413, 344–350.
8. Ding, F.; Xu, W.; Graff, G.L.; Zhang, J.; Sushko, M.L.; Chen, X.; Shao, Y.; Engelhard, M.H.; Nie, Z.; Xiao, J. Dendrite-free lithium deposition via self-healing electrostatic shield mechanism. J. Am. Chem. Soc. 2013, 135, 4450–4456.
9. Zhang, Y.; Qian, J.; Xu, W.; Russell, S.M.; Chen, X.; Nasybulin, E.; Bhattacharya, P.; Engelhard, M.H.; Mei, D.; Cao, R. Dendrite-free lithium deposition with self-aligned nanorod structure. Nano Lett. 2014, 14, 6889–6896.
10. Wan, M.; Kang, S.; Wang, L.; Lee, H.-W.; Zheng, G.W.; Cui, Y.; Sun, Y. Mechanical rolling formation of interpenetrated lithium metal/lithium tin alloy foil for ultrahigh-rate battery anode. Nat. Commun. 2020, 11, 1–10.
11. Pathak, R.; Chen, K.; Gurung, A.; Reza, K.M.; Bahrami, B.; Pokharel, J.; Baniya, A.; He, W.; Wu, F.; Zhou, Y. Fluorinated hybrid solid-electrolyte-interphase for dendrite-free lithium deposition. Nat. Commun. 2020, 11, 1–10.
12. Yang, C.-P.; Yin, Y.-X.; Zhang, S.-F.; Li, N.-W.; Guo, Y.-G. Accommodating lithium into 3D current collectors with a submicron skeleton towards long-life lithium metal anodes. Nat. Commun. 2015, 6, 8058.
13. Lu, L.-L.; Ge, J.; Yang, J.-N.; Chen, S.-M.; Yao, H.-B.; Zhou, F.; Yu, S.-H. Free-standing copper nanowire network current collector for improving lithium anode performance. Nano Lett. 2016, 16, 4431–4437.
14. Yun, Q.; He, Y.B.; Lv, W.; Zhao, Y.; Li, B.; Kang, F.; Yang, Q.H. Chemical dealloying derived 3D porous current collector for Li metal anodes. Adv. Mater. 2016, 28, 6932–6939.
15. Zhao, H.; Lei, D.; He, Y.B.; Yuan, Y.; Yun, Q.; Ni, B.; Lv, W.; Li, B.; Yang, Q.H.; Kang, F. Compact 3D Copper with Uniform Porous Structure Derived by Electrochemical Dealloying as Dendrite-Free Lithium Metal Anode Current Collector. Adv. Energy Mater. 2018, 8, 1800266.
16. An, Y.; Fei, H.; Zeng, G.; Xu, X.; Ci, L.; Xi, B.; Xiong, S.; Feng, J.; Qian, Y. Vacuum distillation derived 3D porous current collector for stable lithium–metal batteries. Nano Energy 2018, 47, 503–511.
17. Zou, P.; Wang, Y.; Chiang, S.-W.; Wang, X.; Kang, F.; Yang, C. Directing lateral growth of lithium dendrites in micro-compartmented anode arrays for safe lithium metal batteries. Nat. Commun. 2018, 9, 464.
18. Wang, S.H.; Yin, Y.X.; Zuo, T.T.; Dong, W.; Li, J.Y.; Shi, J.L.; Zhang, C.H.; Li, N.W.; Li, C.J.; Guo, Y.G. Stable Li metal anodes via regulating lithium plating/stripping in vertically aligned microchannels. Adv. Mater. 2017, 29, 1703729.
19. Li, Q.; Zhu, S.; Lu, Y. 3D porous Cu current collector/Li-metal composite anode for stable lithium-metal batteries. Adv. Funct. Mater. 2017, 27, 1606422.
20. Cao, Z.; Li, B.; Yang, S. Dendrite-Free Lithium Anodes with Ultra-Deep Stripping and Plating Properties Based on Vertically Oriented Lithium–Copper–Lithium Arrays. Adv. Mater. 2019, 31, 1901310.
21. Yan, J.; Yu, J.; Ding, B. Mixed ionic and electronic conductor for Li-metal anode protection. Adv. Mater. 2018, 30, 1705105.
22. Hou, Z.; Yu, Y.; Wang, W.; Zhao, X.; Di, Q.; Chen, Q.; Chen, W.; Liu, Y.; Quan, Z. Lithiophilic Ag nanoparticle layer on Cu current collector toward stable Li metal anode. ACS Appl. Mater. Interfaces 2019, 11, 8148–8154.
23. Cui, S.; Zhai, P.; Yang, W.; Wei, Y.; Xiao, J.; Deng, L.; Gong, Y. Large-Scale Modification of Commercial Copper Foil with Lithiophilic Metal Layer for Li Metal Battery. Small 2020, 16, 1905620.
24. Ma, Y.; Gu, Y.; Yao, Y.; Jin, H.; Zhao, X.; Yuan, X.; Lian, Y.; Qi, P.; Shah, R.; Peng, Y. Alkaliphilic Cu2O nanowires on copper foam for hosting Li/Na as ultrastable alkali-metal anodes. J. Mater. Chem. A 2019, 7, 20926–20935.
25. Wu, S.; Jiao, T.; Yang, S.; Liu, B.; Zhang, W.; Zhang, K. Lithiophilicity conversion of the Cu surface through facile thermal oxidation: Boosting a stable Li–Cu composite anode through melt infusion. J. Mater. Chem. A 2019, 7, 5726–5732.
26. Luan, J.; Zhang, Q.; Yuan, H.; Sun, D.; Peng, Z.; Tang, Y.; Ji, X.; Wang, H. Plasma-Strengthened Lithiophilicity of Copper Oxide Nanosheet–Decorated Cu Foil for Stable Lithium Metal Anode. Adv. Sci. 2019, 6, 1901433.
27. Zhang, Q.; Luan, J.; Tang, Y.; Ji, X.; Wang, S.; Wang, H. A facile annealing strategy for achieving in situ controllable Cu2 O nanoparticle decorated copper foil as a current collector for stable lithium metal anodes. J. Mater. Chem. A 2018, 6, 18444–18448.
28. Zhang, C.; Lv, W.; Zhou, G.; Huang, Z.; Zhang, Y.; Lyu, R.; Wu, H.; Yun, Q.; Kang, F.; Yang, Q.H. Vertically aligned lithiophilic CuO nanosheets on a Cu collector to stabilize lithium deposition for lithium metal batteries. Adv. Energy

Mater. 2018, 8, 1703404.

29. Qin, L.; Xu, H.; Wang, D.; Zhu, J.; Chen, J.; Zhang, W.; Zhang, P.; Zhang, Y.; Tian, W.; Sun, Z. Fabrication of lithiophilic copper foam with interfacial modulation toward high-rate lithium metal anodes. ACS Appl. Mater. Interfaces 2018, 10, 27764–27770.
30. Li, Q.; Pan, H.; Li, W.; Wang, Y.; Wang, J.; Zheng, J.; Yu, X.; Li, H.; Chen, L. Homogeneous interface conductivity for lithium dendrite-free anode. Acs Energy Lett. 2018, 3, 2259–2266.
31. Liu, Y.; Lin, D.; Yuen, P.Y.; Liu, K.; Xie, J.; Dauskardt, R.H.; Cui, Y. An artificial solid electrolyte interphase with high Li-ion conductivity, mechanical strength, and flexibility for stable lithium metal anodes. Adv. Mater. 2017, 29, 1605531.
32. Lei, M.; You, Z.; Ren, L.; Liu, X.; Wang, J.-G. Construction of copper oxynitride nanoarrays with enhanced lithiophilicity toward stable lithium metal anodes. J. Power Sources 2020, 463, 228191.
33. Huang, Z.; Zhang, C.; Lv, W.; Zhou, G.; Zhang, Y.; Deng, Y.; Wu, H.; Kang, F.; Yang, Q.-H. Realizing stable lithium deposition by in situ grown Cu2S nanowires inside commercial Cu foam for lithium metal anodes. J. Mater. Chem. A 2019, 7, 727–732.
34. Zhang, C.; Lyu, R.; Lv, W.; Li, H.; Jiang, W.; Li, J.; Gu, S.; Zhou, G.; Huang, Z.; Zhang, Y. A Lightweight 3D Cu Nanowire Network with Phosphidation Gradient as Current Collector for High-Density Nucleation and Stable Deposition of Lithium. Adv. Mater. 2019, 31, 1904991.
35. Jiang, T.; Chen, K.; Wang, J.; Hu, Z.; Wang, G.; Chen, X.-D.; Sun, P.; Zhang, Q.; Yan, C.; Zhang, L. Nitrogen-doped graphdiyne nanowall stabilized dendrite-free lithium metal anodes. J. Mater. Chem. A 2019, 7, 27535–27546.
36. Zhang, R.; Wen, S.; Wang, N.; Qin, K.; Liu, E.; Shi, C.; Zhao, N. N-Doped Graphene Modified 3D Porous Cu Current Collector toward Microscale Homogeneous Li Deposition for Li Metal Anodes. Adv. Energy Mater. 2018, 8, 1800914.
37. Wang, S.-H.; Yue, J.; Dong, W.; Zuo, T.-T.; Li, J.-Y.; Liu, X.; Zhang, X.-D.; Liu, L.; Shi, J.-L.; Yin, Y.-X. Tuning wettability of molten lithium via a chemical strategy for lithium metal anodes. Nat. Commun. 2019, 10, 1–8.
38. Weng, Y.-T.; Liu, H.-W.; Pei, A.; Shi, F.; Wang, H.; Lin, C.-Y.; Huang, S.-S.; Su, L.-Y.; Hsu, J.-P.; Fang, C.-C. An ultrathin ionomer interphase for high efficiency lithium anode in carbonate based electrolyte. Nat. Commun. 2019, 10, 1–10.
39. Gąsior, W.; Onderka, B.; Moser, Z.; Dębski, A.; Gancarz, T. Thermodynamic evaluation of Cu–Li phase diagram from EMF measurements and DTA study. Calphad 2009, 33, 215–220.
40. Wang, C.; Wang, D.; Dai, C. High-rate capability and enhanced cyclability of rechargeable lithium batteries using foam lithium anode. J. Electrochem. Soc. 2008, 155, A390–A394.
41. Xu, Y.; Menon, A.S.; Harks, P.P.R.; Hermes, D.C.; Haverkate, L.A.; Unnikrishnan, S.; Mulder, F.M. Honeycomb-like porous 3D nickel electrodeposition for stable Li and Na metal anodes. Energy Storage Mater. 2018, 12, 69–78.
42. Chi, S.S.; Liu, Y.; Song, W.L.; Fan, L.Z.; Zhang, Q. Prestoring lithium into stable 3D nickel foam host as dendrite-free lithium metal anode. Adv. Funct. Mater. 2017, 27, 1700348.
43. Jiang, J.; Pan, Z.; Kou, Z.; Nie, P.; Chen, C.; Li, Z.; Li, S.; Zhu, Q.; Dou, H.; Zhang, X. Lithiophilic polymer interphase anchored on laser-punched 3D holey Cu matrix enables uniform lithium nucleation leading to super-stable lithium metal anodes. Energy Storage Mater. 2020, 29, 84–91.
44. Liang, Z.; Lin, D.; Zhao, J.; Lu, Z.; Liu, Y.; Liu, C.; Lu, Y.; Wang, H.; Yan, K.; Tao, X. Composite lithium metal anode by melt infusion of lithium into a 3D conducting scaffold with lithiophilic coating. Proc. Natl. Acad. Sci. USA 2016, 113, 2862–2867.
45. Li, X.; Yang, G.; Zhang, S.; Wang, Z.; Chen, L. Improved lithium deposition on silver plated carbon fiber paper. Nano Energy 2019, 66, 104144.
46. Lu, W.; Wu, C.; Wei, W.; Ma, J.; Chen, L.; Chen, Y. Lithiophilic NiO hexagonal plates decorated Ni collector guiding uniform lithium plating for stable lithium metal anode. J. Mater. Chem. A 2019, 7, 24262–24270.
47. Yue, X.-Y.; Wang, W.-W.; Wang, Q.-C.; Meng, J.-K.; Zhang, Z.-Q.; Wu, X.-J.; Yang, X.-Q.; Zhou, Y.-N. CoO nanofiber decorated nickel foams as lithium dendrite suppressing host skeletons for high energy lithium metal batteries. Energy Storage Mater. 2018, 14, 335–344.
48. Huang, G.; Lou, P.; Xu, G.-H.; Zhang, X.; Liang, J.; Liu, H.; Liu, C.; Tang, S.; Cao, Y.-C.; Cheng, S. Co3O4 nanosheet decorated nickel foams as advanced lithium host skeletons for dendrite-free lithium metal anode. J. Alloy. Compd. 2020, 817, 152753.
49. Sun, C.; Li, Y.; Jin, J.; Yang, J.; Wen, Z. ZnO nanoarray-modified nickel foam as a lithiophilic skeleton to regulate lithium deposition for lithium-metal batteries. J. Mater. Chem. A 2019, 7, 7752–7759.
50. Huang, G.; Chen, S.; Guo, P.; Tao, R.; Jie, K.; Liu, B.; Zhang, X.; Liang, J.; Cao, Y.-C. In Situ Constructing Lithiophilic NiFx Nanosheets on Ni Foam Current Collector for Stable Lithium Metal Anode via a Succinct Fluorination Strategy.

Chem. Eng. J. 2020, 395, 125122.

51. Zhu, J.; Chen, J.; Luo, Y.; Sun, S.; Qin, L.; Xu, H.; Zhang, P.; Zhang, W.; Tian, W.; Sun, Z. Lithiophilic metallic nitrides modified nickel foam by plasma for stable lithium metal anode. Energy Storage Mater. 2019, 23, 539–546.
52. Zhu, R.; Zhu, C.; Sheng, N.; Rao, Z.; Aoki, Y.; Habazaki, H. A widely applicable strategy to convert fabrics into lithiophilic textile current collector for dendrite-free and high-rate capable lithium metal anode. Chem. Eng. J. 2020, 388, 124256.
53. Wu, S.; Zhang, Z.; Lan, M.; Yang, S.; Cheng, J.; Cai, J.; Shen, J.; Zhu, Y.; Zhang, K.; Zhang, W. Lithiophilic Cu-CuO-Ni Hybrid Structure: Advanced Current Collectors toward Stable Lithium Metal Anodes. Adv. Mater. 2018, 30, 1705830.
54. Lu, W.; Wu, C.; Wei, W.; Ma, J.; Chen, L.; Chen, Y. Lithiophilic NiO hexagonal plates decorated Ni collector guiding uniform lithium plating for stable lithium metal anode. J. Mater. Chem. A 2019, 7, 24262–24270
55. Pathak, R.; Chen, K.; Gurung, A.; Reza, K.M.; Bahrami, B.; Wu, F.; Chaudhary, A.; Ghimire, N.; Zhou, B.; Zhang, W.H. Ultrathin bilayer of graphite/SiO2 as solid interface for reviving Li metal anode. Adv. Energy Mater. 2019, 9, 1901486.
56. Xie, K.; Wei, W.; Yuan, K.; Lu, W.; Guo, M.; Li, Z.; Song, Q.; Liu, X.; Wang, J.-G.; Shen, C. Toward dendrite-free lithium deposition via structural and interfacial synergistic effects of 3D graphene@ Ni scaffold. ACS Appl. Mater. Interfaces 2016, 8, 26091–26097.
57. Ye, H.; Xin, S.; Yin, Y.-X.; Li, J.-Y.; Guo, Y.-G.; Wan, L.-J. Stable Li plating/stripping electrochemistry realized by a hybrid Li reservoir in spherical carbon granules with 3D conducting skeletons. J. Am. Chem. Soc. 2017, 139, 5916–5922.
58. Kang, H.-K.; Woo, S.-G.; Kim, J.-H.; Lee, S.-R.; Lee, D.-G.; Yu, J.-S. Three-dimensional monolithic corrugated graphene/Ni foam for highly stable and efficient Li metal electrode. J. Power Sources 2019, 413, 467–475.
59. Zhang, X.; Wang, A.; Lv, R.; Luo, J. A corrosion-resistant current collector for lithium metal anodes. Energy Storage Mater. 2019, 18, 199–204.
60. Huang, K.; Li, Z.; Xu, Q.; Liu, H.; Li, H.; Wang, Y. Lithiophilic CuO Nanoflowers on Ti-Mesh Inducing Lithium Lateral Plating Enabling Stable Lithium-Metal Anodes with Ultrahigh Rates and Ultralong Cycle Life. Adv. Energy Mater. 2019, 9, 1900853.
61. Lee, H.; Song, J.; Kim, Y.-J.; Park, J.-K.; Kim, H.-T. Structural modulation of lithium metal-electrolyte interface with three-dimensional metallic interlayer for high-performance lithium metal batteries. Sci. Rep. 2016, 6, 1–10.
